3D constrained inversion of CSEM data with acoustic velocity using full waveform inversion

Nuno Vieira da Silva[1], *Joanna Morgan*[1], *Mike Warner*[1], *Adrian Umpleby*[1], *Ivan Stekl*[1]
[1]*Formerly Imperial College London, presently CGGVeritas R&D (UK)*
[2]*Imperial College London*

SUMMARY

The marine Controlled Source Electromagnetic Method (CSEM) has been used as exploration technology in the oil and gas industry. Inversion is the most widely used technique for interpretation of electromagnetic data. Nonetheless, resistivity images obtained from CSEM data generally have low resolution creating difficulties in the accurate characterization of geological reservoirs (containing hydrocarbons or for CO_2 storage for example). Here is shown that by integrating a velocity field to guide the CSEM inversion leads to better focused resistivity images reducing ambiguities and source-receiver footprint. The proposed method integrates velocity models obtained through seismic full waveform inversion, in a constrained inversion algorithm for controlled source electromagnetic data. A synthetic example using a modified version of the Marmousi model is presented to validate the proposed methodology.

INTRODUCTION

During the past ten years the marine CSEM data has been acquired in commercial surveys (Ellingsrud, 2002). The change by several orders of magnitude of the resistivity of geological formations when the pores are filled with oil or gas in comparison to when they are filled with brine makes it of particular importance as a de-risking method, especially when complementing the more widely used seismic reflection method. However, marine CSEM struggles to deliver high resolution images. First, because both the solid earth and sea-water are conductive, and therefore the electromagnetic field propagates in the diffusive regime. Secondly, the inherently ill-posedness of the CSEM inversion requires the use of constraints in the model parameter space by imposing smooth variation of the model parameters or of its derivatives. This process is known as the regularization of the inverse problem (Zhdanov, 2002), and generally leads to underestimated and poorly spatially constrained resistivity models, i.e. the inverted anomalies are generally larger than their actual dimension, and tend to be mispositioned. It is well known that this problem can be mitigated by integrating different data spaces in the inversion, being this approach also known as joint inversion. Seismic imaging generally delivers higher resolution images when compared to electromagnetic methods, and therefore inversion of CSEM data constrained with seismic data leads, in principle, to better focused electromagnetic images. However, it is important to note that not all kinds of seismic inversion deliver high resolution images. For example, travel time tomography also delivers low resolution images as it is mainly sensitive to the long wavelengths of the velocity anomalies, in contrast to the full waveform inversion (FWI) which can deliver high resolution velocity models. This makes FWI the best candidate for constraining CSEM inversion. However, the FWI problem is highly non-linear and requires a starting model very close to the true model of velocity, as it is sensitive to cycle skipping and thereby prone to converge to local minima. This problem is aggravated with increasing frequency, being this the reason why it requires the use of low frequencies in the data. With improved computational capabilities and algorithmic approaches, the FWI is becoming increasingly used for seismic exploration of hydrocarbons, and therefore the integration of seismic data for driving CSEM inversion is a possibility where seismic and CSEM surveys have been carried out aiming to image the same geological target. However both the 3D FWI and CSEM inversion are computationally very intensive, as generally are estimated a few millions of model parameters in each model parameter space. In addition, the use of the Hessian in order to accelerate the solution of the inverse problem can also increase the computational load dramatically. Thus even with modern distributed computing systems with a few tens of GB per node and interconnected with a high speed network, may still be challenging to run full 3D joint inversions. This problem can, in principle, be mitigated by alternating the electromagnetic and seismic inversion iterations at each joint inversion iteration. For example Hu et al. (2009) used this approach for 2D joint inversion of electromagnetic and seismic data. Here we present an approach that integrates a priori inverted velocity models in the CSEM inversion through the use of an additional regularization term in the objective function. Rather than inverting seismic and CSEM data in a unified inversion scheme, it uses the structural information of the velocity model in order to impose spatial constraints to the resistivity image. The extra regularization term is the cross product of the gradients of the acoustic velocity and of the logarithm of resistivity in the three-dimensional space. As the seismic inversion and resistivity inversion grids are not the same, and the resistivity grid is coarser than the seismic inversion grid, it is used a mapping operator from the seismic inversion grid into the resistivity inversion grid, for the computation of the structural constraining term. In the next sections is described the approach for constrained inversion of CSEM data, and an example is shown for its validation.

FULL WAVEFORM INVERSION

FWI attempts to determine a velocity model which minimizes the misfit between seismic field data and synthetic data. The FWI algorithm used here uses a time domain engine, and the numerical solution is obtained using the finite difference method with a fourth order approximation in space and a second order approximation in time. For a more complete description refer to Warner (2010). The utilized FWI code allows for Vertical Transverse Isotropy (¿VTI), however, in this work are only

DOI http://dx.doi.org/10.1190/segam2012-1449.1

considered isotropic velocity models. The objective function for FWI is measured using the L_2 norm:

$$J = \|\mathbf{C}\delta\mathbf{d}_S\|_2^2 \quad (1)$$

Where $\delta\mathbf{d}_S$ is the seismic data misfit and $\mathbf{C}$ is a weighting matrix. The optimal velocity model is approximated using the linearized updating expression for slowness:

$$\mathbf{s}_{k+1} = \mathbf{s}_k - \alpha_k \mathbf{H}_k^{-1} \nabla J_k \quad (2)$$

Where $\mathbf{s}_k$ is the slowness at the k-th iteration, α_k is the step length which is determined by a line search method and $\mathbf{H}_k$ is an approximation of the diagonal of the Hessian of the objective function for the full waveform inversion problem at the k-th iteration (Pratt, 1998). The gradient of 1 is computed using the adjoint state method (Plessix, 2006).

CONSTRAINED INVERSION OF CSEM

The presented constrained inversion (CI) algorithm uses a velocity model that has been inverted prior to run the CSEM inversion. Thereby this approach is completely general and allows the integration of any velocity models which are available for imaging the same geological structures. As the velocity model is kept constant during the inversion, the only contribution for changes in the structural regularizing term come from the successive updates in the resistivity model. The solution of the CI problem is obtained through the solution of the optimization problem:

$$\min_m f = \quad (3)$$

$$\min_m = \|\mathbf{W}\delta\mathbf{d}_{EM}\|_2^2 + \lambda\|\mathbf{L}\mathbf{m}\|_2 + \beta\sum_{i=1}^{N_m}\|\nabla v_i \times \nabla m_i\|_2^2$$

Where $\delta\mathbf{d}_{EM}$ is the misfit of the electromagnetic data, $\mathbf{W}$ is a weighting matrix based on the amplitude of the field data or on the standard deviation of the data, $\mathbf{L}$ is a discretization of a second order operator, $\mathbf{m}$ is the logarithm of the conductivity, v_i is the velocity for the i-th inversion cell, m_i is the logarithm of the conductivity for the i-th inversion cell, N_m is the number of model parameters to be estimated, λ and β are regularization parameters and weight the constraining terms in the objective function. The regularization parameter λ is determined using a cooling approach (Farquharson,2004), and the structural weighting parameter beta is determined using a fraction of the summed contributions of data misfit and of the smoothing constraining term to the objective function. The structural weighting parameter is determined on an experimental basis for each case.

The solution of ref(eq:functional) is obtained using the linearized iterative updating expression:

$$\mathbf{m}_{k+1} = \mathbf{m}_k - \alpha_k \mathbf{H}_k^{-1} \nabla f_k \quad (4)$$

The inverse of the Hessian, $\mathbf{H}_k$, is approximated using the L-BFGS method (Nocedal, 2006), and the gradient is computed using the adjoint method (McGillivray, 1994). The field and adjoint field responses are computed using a forward modeling engine for three-dimensional CSEM forward modeling in the frequency domain, using edge finite elements (Vieira da Silva, 2012).

SYNTHETIC MODEL EXAMPLE

Here is presented an example which validates the 3D CSEM constrained inversion algorithm. In this example it is used a modified version of the Marmousi model, where two velocity anomalies are added, and the sea-bottom is deeper than in the original model. Figure 1 shows a slice of the true velocity model in the plan y = 0 m. The seismic synthetic data was generated discretizing the true velocity model using a $384 \times 83 \times 125$ grid, equally spaced 24 m in all the three Cartesian directions. The seismic traces were simulated for 93 sources and are recorded at 2159 receivers equally spaced in the grid, and are sampled at each 2 ms and have a length of 6 s. The inversion is carried out for four frequencies: 4, 5, 6 and 7 Hz, and five iterations per frequency, totalizing 20 iterations, as the multi-scale approach is used in order to mitigate the existence of local minima (Bunks, 1995). The starting model is a smoothed model built from the true model. Figure 2 shows a slice of the inverted velocity model in the plan y = 0 m. The

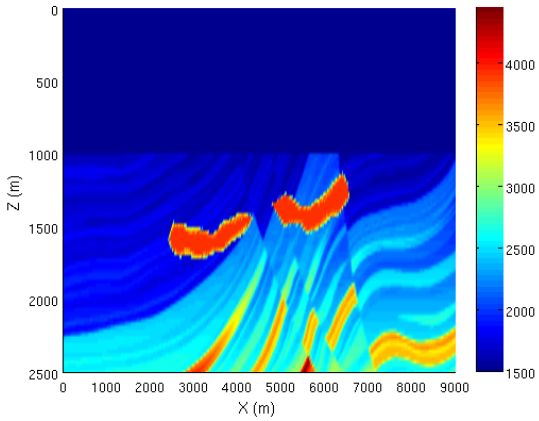

Figure 1: Slice of the original velocity model at y = 0. Colorbar units are in m/s.

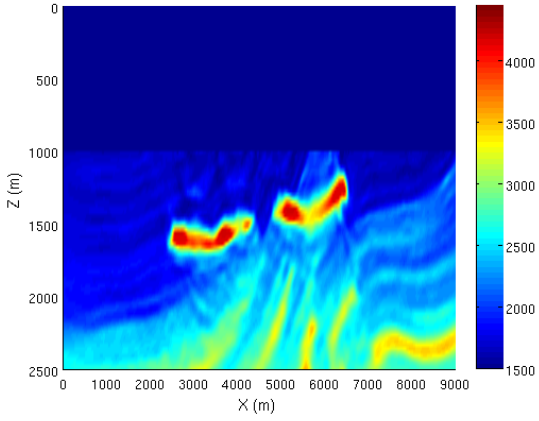

Figure 2: Slice of the inverted velocity model at y = 0. Colorbar units are in m/s.

DOI http://dx.doi.org/10.1190/segam2012-1449.1

CSEM synthetic data is computed using the resistivity model shown in figure 3. The synthetic resistivity model presents two resistive anomalies over a background of 1 Ωm, and the sea-water is 0.33 and 1000 m deep. The simulation grid is (dimension grid) and the grid spacing ranges between 20 and 80 m. The synthetic data is simulated discretizing the true resistivity model with a $177 \times 139 \times 33$ irregularly space, with grid spacing ranging between 20 and 120 m. The data is generated for 15 sources and recorded at 54 receivers, and for two frequencies: 0.5 and 1.0 Hz. For the inversion it is added 3 % of Gaussian noise to the synthetic data. The CSEM inversion is carried out using a smoothing constraining only and using the additional structural term. The starting model for both inversions is a homogeneous background of 1 Ωm, and the inversion grid is decoupled from the modeling grid in order to mitigate the existence of redundant parameters due to the forward modeling grid refinement in the vicinity of electromagnetic sources and receivers. The grid spacing for the inversion grid ranges between 40 and 100 m. Figure 5 shows a slice the inverted resistivity model in the plan y = 0 m, using the smoothing constraint only. The inversion takes 26 iterations to decrease the synthetic data misfit by 74 %. For carrying out the structural constrained inversion, the inverted velocity model (figure 2), is mapped into the inversion grid using a weighted mapping operator which takes into account the values of the velocity model for several cells in the neighborhood of the point of interest in the resistivity inversion grid. Figure 4 shows the inverted velocity model, after applying the projection operator over the velocity model. The mapped velocity model used for the structural constraint has a blocky aspect as the CHEM inversion grid is coarser than the grid used for FWI. The weighting parameter is set 0.5 and the constrained inversion algorithm takes 198 iterations for the synthetic data misfit to decrease 72 %. Figure 6 shows a slice of the inverted resistivity model using the structural constraint in the plan y = 0 m. Comparing figures 5 and 6, one can conclude that indeed the structural constraint leads to a better focused image, and reduces ambiguity , as for instance when using conventional migration the shallower anomaly is reconstructed in two

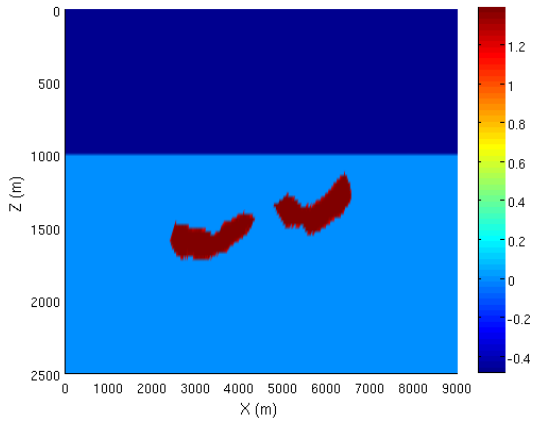

Figure 3: Slice of the original resistivity model at y = 0 m. Colorbar units are in Log_{10} [Ωm].

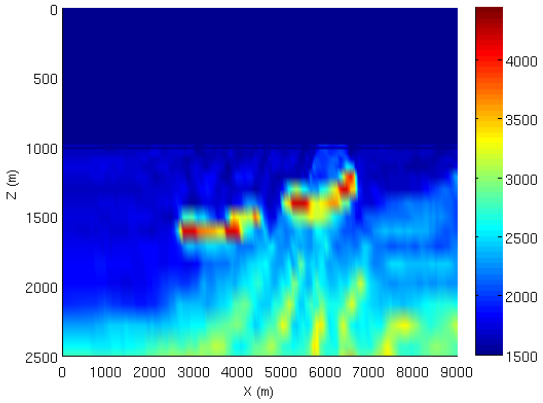

Figure 4: Slice of the mapped velocity model. Colorbar units are in in m/s.

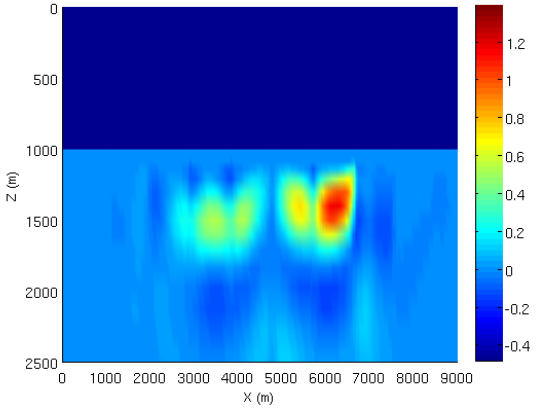

Figure 5: Slice of the inverted resistivity model using smoothing constraints only, at y = 0 m. Colorbar units are in Log_{10} [Ωm].

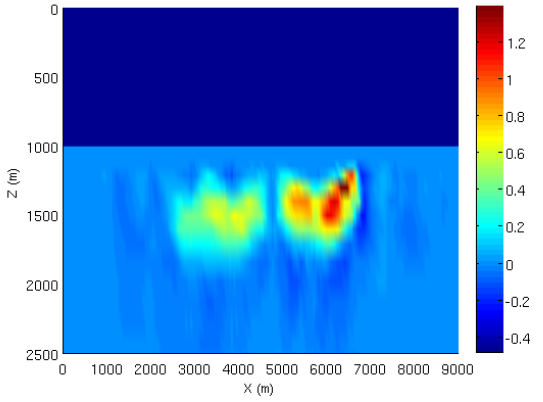

Figure 6: Slice of the inverted resistivity model using structural constraints only, at y = 0 m. Colorbar units are in Log_{10} [Ωm].

DOI http://dx.doi.org/10.1190/segam2012-1449.1

regions, this is due to the source-receiver foot print. In the case of constrained inversion the same anomaly is reconstructed as an entire body and the geometrical shape is better defined. The resistivity values of the deeper anomaly are better determined using the presented constraining method.

CONCLUSIONS

It was presented an algorithm for 3D constrained inversion of CSEM data using a velocity model determined from FWI to build a regularizing structural term. The structural term is based on the well-known method of cross product of gradients of the complementary model parameters in the three-dimensional space. As shown, this simple yet useful approach is capable of improving the focusing of inverted resistivity models. The presented algorithm for constrained inversion has the advantage of being entirely flexible, and not only can be used to integrate any available velocity models, but it can also be used to integrate any other parameter defining spatial structure. In fact, v in equation 4 can represent gravity, reflectivity, etc. The only necessary condition is that the parameter defining structure must have a continuous distribution is space in order to compute the term ∇v. The scalability of the constrained inversion algorithm is essentially determined by the forward modeling solver which uses a multifrontal method. Further improvements of the forward solver, should allow for very large scale problems and data sets to be considered with the presented approach. Even though not shown here, we speculate that this method is also valid for resistivity models with anisotropy and therefore future research will be oriented for the extension of the presented constrained inversion algorithm to the case of constrained inversion for anisotropic resistivity.

ACKNOWLEDGMENTS

The first author was supported by Fundacao para a Ciencia e Tecnologia (FCT) research grant SFRH/BD/40809/2007. This work was developed in the scope of the FULLWAVE III consortium, consisting of BG, BP, Chevron, ConocoPhillips, ENI, Maersk, Nexen, OHM, Rio Tinto, CGGVeritas and the U.K. Dept. for B.I.S, under the IT programme

http://dx.doi.org/10.1190/segam2012-1449.1

EDITED REFERENCES

Note: This reference list is a copy-edited version of the reference list submitted by the author. Reference lists for the 2012 SEG Technical Program Expanded Abstracts have been copy edited so that references provided with the online metadata for each paper will achieve a high degree of linking to cited sources that appear on the Web.

REFERENCES

Carey, B., F. M. Saleck, S. Zaleski, and G. Chavent, 1995, Multiscale seismic waveform inversion: Geophysics, **60**, 1457–1473.

Ellingsrud, S., T. Eidesmo, S. Johansen, M. Sinha, L. MacGregor, and S. Constable, 2002, The meter reader-remote sensing of hydrocarbon layers by seabed logging (SBL): Results from a cruise offshore Angola: The Leading Edge, **21**, 972–982.

Farquharson, C., and D. W. Oldenburg, 2004, A comparison of automatic techniques for estimating the regularization parameter in non-linear inverse problems: Geophysical Journal International, **156**, 411–425.

McGillivray, P. R., D. W. Oldenburg, R. G. Ellis, and T. M. Habashy, 1994, Calculation of sensitivities for the frequency-domain electromagnetic problem: Geophysical Journal International, **116**, 1–4.

Nocedal, J., and S. J. Wright, 2006, Numerical optimization, 2nd ed.: Springer.

Plessix, R. E., 2006, A review of the adjoint-state method for computing the gradient of a functional with geophysical applications: Geophysical Journal International, **167**, 495–503.

Pratt, G., C. Shin, and G. J. Hicks, 1998, Gauss-Newton and full Newton methods in frequency-space seismic waveform inversion: Geophysical Journal International, **133**, 341–362.

Vieira da Silva, N., J. Morgan, L. MacGregor, and M. Warner, 2012, A finite element multifrontal method for three-dimensional CSEM modeling in the frequency domain: Geophysics, **77**, no. 2, E101–E115.

Warner, M., A. Umpleby, I. Stekl, and J. Morgan, 2010, 3D full-wavefield tomography: Imaging beneath heterogeneous overburden: 72nd Conference and Exhibition, EAGE, Workshops and Fieldtrips, WS6.

Zhdanov, M. S., 2002, Geophysical inverse theory and regularization of inverse problems: Elsevier.